Supporting Information

Carroll et al. 10.1073/pnas.0910128106

SI Text

Adaptive Optics Retinal Imaging. The subjects' right eye was dilated and accommodation suspended using one drop each of phenylephrine hydrochloride (2.5%) and tropicamide (1%). An AO ophthalmoscope was used to obtain images of the cone mosaic. The system at the Medical College of Wisconsin measured the eye's monochromatic aberrations over a 6.8-mm pupil with a Shack-Hartmann wavefront sensor in a continuous closed-loop fashion and corrected for them with a 52-channel deformable mirror (Imagine Eyes). Details on the Mirao52 deformable mirror have been previously published (1). Once a wavefront correction was obtained, a retinal image was acquired by illuminating the retina with a 1.8° diameter, 500-ms flash. A fiber-coupled near infrared source was used for imaging, which consists of a 200-mW SLD (center wavelength of 837.8 nm, 14.1-nm spectral bandwidth FWHM) and 110-m multimode step index fiber (Fiberguide Industries). The optical role of the fiber was to reduce the spatial coherence of the laser and prevent speckle noise that confounds interpretation of the retinal image. A back-illuminated scientific-grade 12-bit charge-coupled device (CCD), the Cam1M100-SFT (Sarnoff Corporation), captured images of the retina. During each exposure, continuous images of the retina were collected at a frame rate of 167 fps with 6-ms exposure.

The University of Rochester AO system also measured the eye's monochromatic aberrations over a 6.8-mm pupil with a Shack-Hartmann wavefront sensor, however a 97-channel deformable mirror (Xinetics) was used for correction. Upon wavefront correction, a retinal image was acquired by illuminating the retina with a 1° diameter, 4-ms flash [650 or 550 nm, 40-nm bandwidth (full width at half max)] from a krypton arc flash lamp. Individual images were taken with a CCD (Roper Scientific). Details on this system have been published, see ref. 2. For both systems, a paper fixation target placed within the optical system was used to guide the retinal location being imaged.

Molecular Genetics. DNA was extracted from whole blood obtained from all nine color deficient subjects (3) and used in a previously described real-time quantitative PCR assay to estimate the relative number of L and M genes in the X-chromosome visual pigment gene array (4). For eight of the subjects, the L and M genes were selectively amplified by long-distance PCR, and the product obtained was subsequently used to amplify separately exons 2, 3, and 4 of L and of M genes for direct DNA sequence analysis (sequencing not done for 6336). The primers and thermal cycling parameters for all amplifications were reported in ref. 5. The resultant PCR products were directly sequenced with the AmpliTaq FS sequencing kit (Applied Biosystems), and sequencing analysis was done with the ABI 310 genetic analyzer.

To determine the position within the array of the gene containing the C203R mutation for subjects 4511 and 4515, long-distance PCR was performed to specifically and separately amplify the first and last genes in the array, as described in refs. 6 and 7. Exon 4 from the first and last genes was directly sequenced as described in ref. 5.

1. Fernández EJ, et al. (2006) Adaptive optics with a magnetic deformable mirror: Applications in the human eye. *Opt Express* 14:8900–8917.
2. Hofer H, et al. (2001) Improvement in retinal image quality with dynamic correction of the eye's aberrations. *Opt Express* 8:631–643.
3. Neitz M, Neitz J, Grishok A (1995) Polymorphism in the number of genes encoding long-wavelength sensitive cone pigments among males with normal color vision. *Vision Res* 35:2395–2407.
4. Neitz M, Neitz J (2001) A new mass screening test for color-vision deficiencies in children. *Color Res Appl* 26:S239–S249.
5. Carroll J, McMahon C, Neitz M, Neitz J (2000) Flicker-photometric electroretinogram estimates of L:M cone photoreceptor ratio in men with photopigment spectra derived from genetics. *J Opt Soc Am A Opt Image Sci Vis* 17:499–509.
6. Hayashi T, Motulsky AG, Deeb SS (1999) Position of a 'green-red' hybrid gene in the visual pigment array determines color-vision phenotype. *Nat Genet* 22:90–93.
7. Kainz PM, Neitz M, Neitz J (1998) Molecular genetics detection of female carriers of protan defects. *Vision Res* 38:3365–3369.
8. Wissinger B, Papke M, Tippmann S, Kohl S (2006) Genotypes in blue cone monochromacy. *Invest Ophthalmol Vis Sci* 47:Abstract 4609.
9. Ueyama H, et al. (2002) Novel missense mutations in red/green opsin genes in congenital color-vision deficiencies. *Biochem Biophys Res Commun* 294:205–209.
10. Neitz M, et al. (2004) Variety of genotypes in males diagnosed as dichromatic on a conventional clinical anomaloscope. *Vis Neurosci* 21:205–216.
11. Winderickx J, et al. (1992) Defective colour vision associated with a missense mutation in the human green visual pigment gene. *Nat Genet* 1:251–256.
12. Ueyama H, et al. (2004) Analysis of L-cone/M-cone visual pigment gene arrays in Japanese males with protan color-vision deficiency. *Vision Res* 44:2241–2252.
13. Nathans J, et al. (1993) Genetic heterogeneity among blue-cone monochromats. *Am J Hum Genet* 53:987–1000.
14. Stenkamp RE, Filipek S, Driessen CAGG, Teller DC, Palczewski K (2002) Crystal structure of rhodopsin: A template for cone visual pigments and other G protein-coupled receptors. *Biochim Biophys Acta* 1565:168–182.

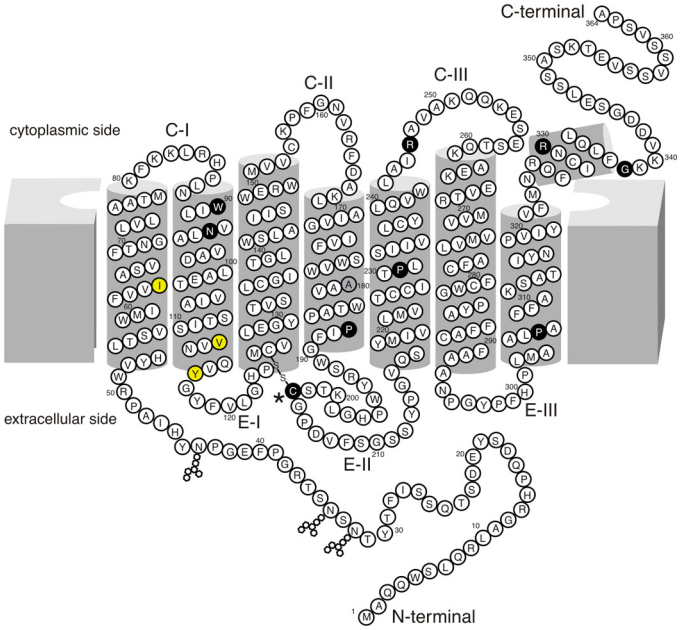

Fig. S1. Two-dimensional diagram of the human M opsin. Each circle represents a single amino acid, with mutations associated with the loss of L or M pigment function shown as filled black circles (C203R mutation denoted with an asterisk). The nine missense mutations reported in the L/M opsins are: W90X (8), N94K, R330Q, and G338E (9), P187S (10), C203R (11), P231L (12), and R247X and P307L (13). The three yellow filled circles are the locations of observed exon 2 polymorphisms in the protan subjects, the filled gray circle is the location of the common S180A polymorphism. Modified from ref. 14 with permission.

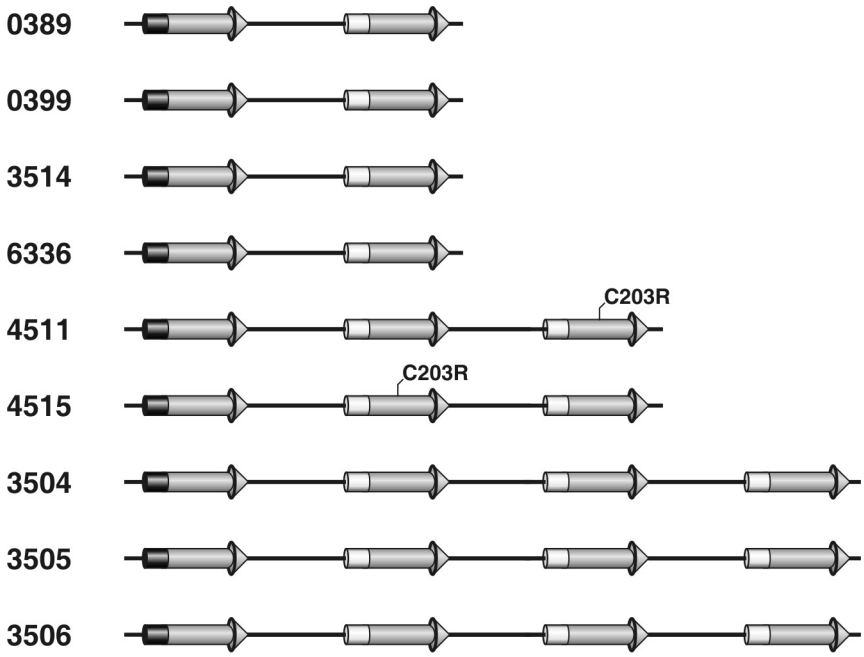

Fig. S2. Schematic representation of the X-encoded photopigment gene array for the subjects examined in this study. All subjects had no L-pigment genes in their arrays, predictive of a protan phenotype, and all except 0399 and 3514 had polymorphisms encoded by exon 2 that would be predicted to introduce a small spectral shift in the λ_{max} or optical density of the corresponding pigment. No sequence data were available for 6336, although he is thought to have polymorphism at multiple sites given his extremely mild protanomalous phenotype. Subjects 4511 and 4515 were each found to have one gene encoding an M pigment with the C203R mutation.

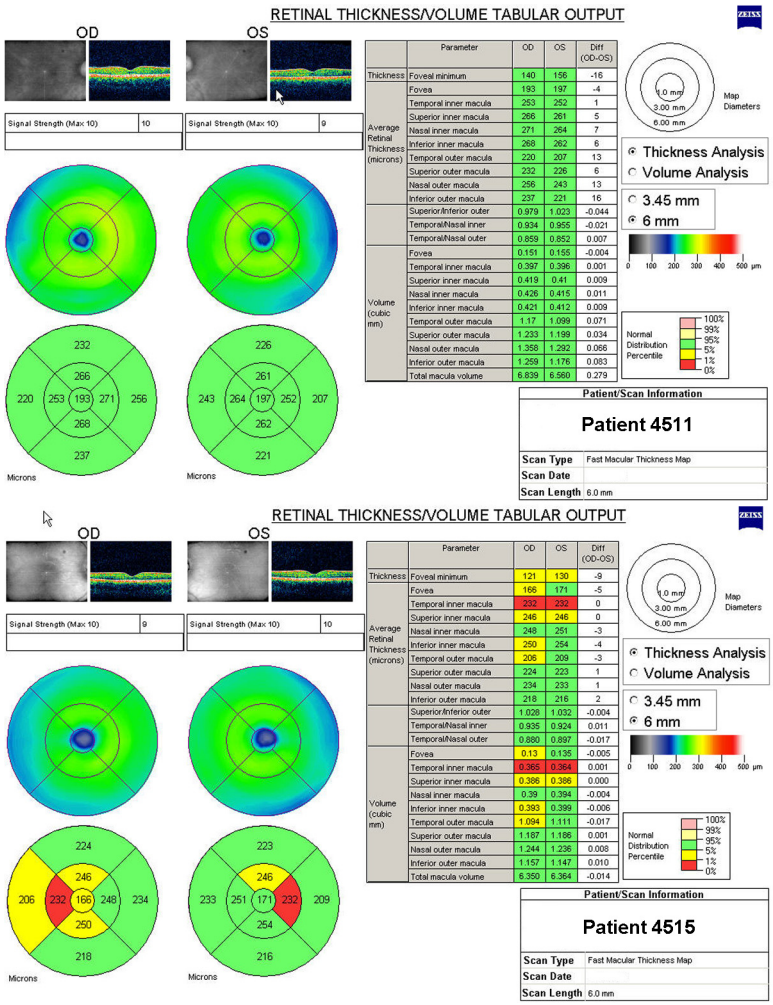

Fig. S3. Macular thickness maps obtained with Stratus (Carl Zeiss Meditec) time-domain OCT. Top panel is from subject 4511 and the bottom panel is from subject 4515. Subtle thinning was seen in subject 4515, whereas macular thickness was within 2 SD of the mean for all nine sectors of the map for subject 4511.

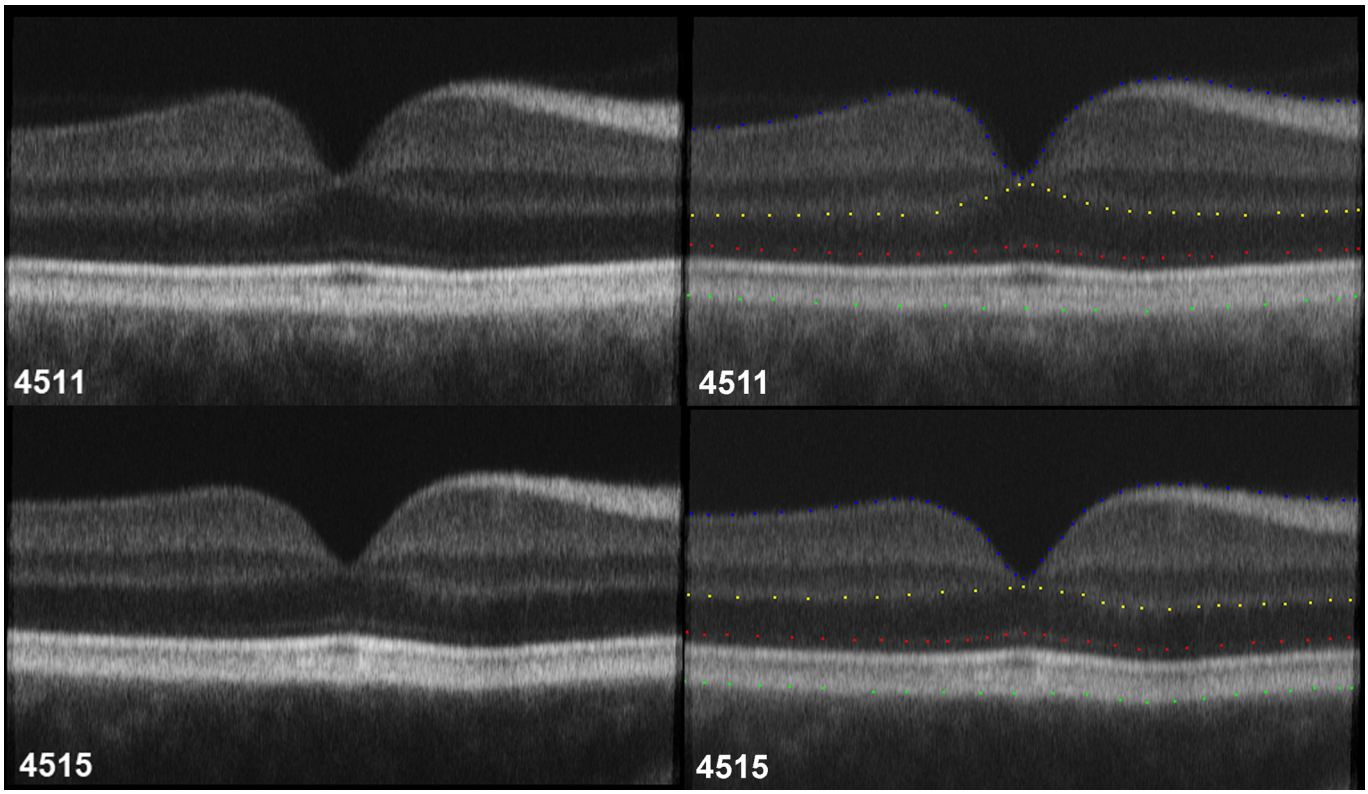

Fig. S4. Segmentation of OCT images from the C203R retina. Shown on the left are the OCT scans used for segmenting total retinal thickness and outer nuclear layer (ONL) thickness. Scans were generated by registering and averaging 10 individual line scans from the Stratus (Carl Zeiss Meditec) time-domain OCT (see text for registration methods). On the right are actual segmentation points used to derive the thickness plots.

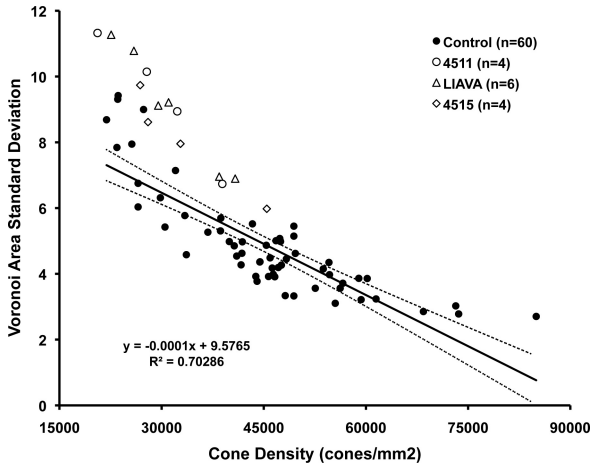

Fig. S5. Voronoi area standard deviation as a function of cone density. Number of points reflect the number of retinal locations tested. Solid line is a least-squares linear regression. Color deficient subjects are plotted as open symbols, and for normal mosaics of the same density, these subjects have more irregular cone packing, as they fall outside of the 95% confidence interval (dashed lines).